DOI: 10.1002/chem.200600478

Predicting the Activity of Single Isolated Lewis Acid Sites in Solid Catalysts

Mercedes Boronat,[a] Avelino Corma,*[a] Michael Renz,[a] and Pedro M. Viruela[b]

Abstract: An experimental study of the activity of Ti-, Zr- and Sn-beta catalysts in different types of oxidation reactions is combined with a quantum-chemical analysis of the electronic properties of the active sites and the adsorbed reactants. The differences observed in the catalytic behaviour of the three materials are explained in terms of the molecular orbital distribution of each system. The intrinsic Lewis acid strength of the isolated active site, the degree of back-donation from the catalyst to the empty orbitals of the organic reactant and the net atomic charges on selected atoms are proposed as predictors of reactivity.

Keywords: catalytic activity · density functional calculations · Lewis acids · oxidation · zeolites

Introduction

The development of isolated and well-defined single-site Lewis acid solid catalysts that are active and selective for new environmentally friendly chemical processes is an urgent need and a challenging scientific target.[1,2] The discovery of Ti silicalite (TS-1) as a catalyst for a series of oxidation reactions and its successful industrial implementation represented an important breakthrough in the use of Lewis acids as heterogeneous catalysts.[3,4] The oxidation properties of TS-1, which can selectively catalyse reactions such as alcohol and alkane oxidation, olefin epoxidation, hydroxylation of aromatics, and cyclohexanone ammoximation, are related to the presence of isolated tetrahedral Ti^{IV} atoms in framework positions. Ti has also been incorporated into the framework of larger-pore 12-ring zeolites[5,6] and into mesoporous molecular sieves.[7] The successful catalytic results obtained with Ti zeolites led to the synthesis of zeolites containing other transition metals in framework positions. Tin and zirconium have been incorporated tetrahedrally into the framework of zeolite beta[8–10] and interesting catalytic properties, different from those of Ti zeolites, have been observed in the products. For instance, Sn-beta is able to perform the chemoselective Baeyer–Villiger oxidation of ketones and aldehydes,[9,11] whereas Ti- or Zr-beta is not. On the other hand, Ti-, Sn- and Zr-beta are all active catalysts for the Meerwein–Ponndorf–Verley reduction of cyclohexanone with 2-butanol, but their activities differ.

The catalytic activity of a Lewis acid for oxidation is related to its ability to form acid–base adducts with either the substrate or the oxidizing agent, enhancing its reactivity. In contrast to Brönsted acidity, however, it is very difficult to define and quantify Lewis acidity. The formation of an adduct implies that an electron density transfer from the Lewis base to the Lewis acid occurs which is directly proportional to the energy difference and degree of overlap between the occupied orbitals of the base and the empty orbitals of the acid. Therefore, the strength of a Lewis acid could be related to the energy of its LUMO in such a way that the lower the LUMO energy, the easier its interaction with a base molecule. However, other factors influence the acid–base interaction: for example, the HSAB (hard–soft acid–base) principle, which states that hard acids coordinate preferentially to hard bases and soft acids with soft bases.[12] Another factor to be considered is the possibility of electron density back-donation from the Lewis acid to the unoccupied orbitals of the Lewis base, an interaction that may or may not occur, depending on the energy difference and degree of overlap between the orbitals involved. Modification of the electronic levels of both the metal and the molecule, by adsorption of a molecule on the metal centre, should also be taken into account; consequently the activity

[a] Dr. M. Boronat, Prof. Dr. A. Corma, Dr. M. Renz
Instituto de Tecnología Química, UPV-CSIC
Universidad Politécnica de Valencia
Av. de los Naranjos, s/n, 46022 Valencia (Spain)
Fax: (+34) 963-877-809
E-mail: acorma@itq.upv.es

[b] Prof. Dr. P. M. Viruela
Institut de Ciència Molecular, Universitat de Valencia
Polígono la Coma s/n, 46980 Paterna (Spain)

Supporting information for this article is available on the WWW under http://www.chemeurj.org/ or from the author.

of a catalyst for a given reaction depends not only on the properties of the isolated active site, but also on the changes caused by its interaction with the reactant molecules.

With all these variables in mind, we have tried to determine the key factors influencing the activity of Ti-, Zr- and Sn-beta in different types of oxidation reactions. In this work we have combined an experimental study of the activity of Ti-, Zr- and Sn-beta catalysts for different reactions with a quantum chemical analysis of the electronic properties of the isolated active sites and the initial reactant com-

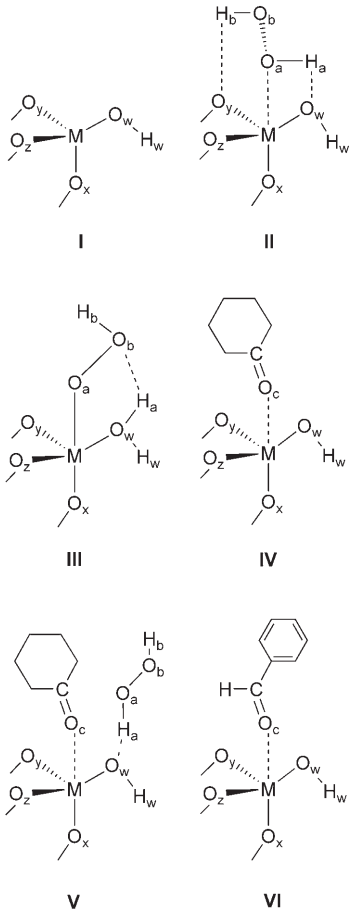

Figure 1. Schematic structures and atom labelling for the catalyst active site (**I**), hydrogen peroxide adsorption complex (**II**), metal–hydroperoxo species active for the epoxidation reaction (**III**), cyclohexanone adsorption complex (**IV**), complex of cyclohexanone and hydrogen peroxide reactants for the Baeyer–Villiger reaction (**V**), and benzaldehyde adsorption complex (**VI**).

plexes shown in Figure 1. The objective is to explain the differences observed in the catalytic behaviour of the three materials in terms of the molecular orbital distribution of each system, and to find the properties or parameters that can be used as reliable descriptors/predictors of reactivity. These parameters will allow us to estimate whether a catalyst may be active for a given reaction, information that can be helpful at an early stage of catalyst selection.

Results and Discussion

Catalytic performance: The behaviour Ti-beta, Zr- and Sn-beta catalysts has been studied experimentally by measuring the initial rates of the Baeyer–Villiger (BV) oxidation of cyclohexanone with H_2O_2, the Meerwein–Ponndorf–Verley (MPV) reduction of cyclohexanone and benzaldehyde with 2-butanol, the epoxidation of octene and the oxidation of diphenyl sulfide (Table 1).

Table 1. Initial rates for the different catalysts employed in the Baeyer–Villiger (BV) oxidation of cyclohexanone, the Meerwein–Ponndorf–Verley (MPV) reductions of cyclohexanone and benzaldehyde in the presence of 2-butanol, epoxidation of octene and oxidation of diphenyl sulfide.

	Initial rate [mmol h^{-1} (g cat)$^{-1}$]		
Reaction	Ti-beta	Zr-beta	Sn-beta
BV, cyclohexanone	0.0[b]	4.71[b]	26.8[b]
MPV, cyclohexanone	0.4[b]	65.6[b]	295[b]
MPV, benzaldehyde	0.2[b]	36.6[b]	10.7[b]
epoxidation, octene	11.0[c]	0.0[b]	0.0[b]
oxidation, sulfide[d]	122 (97:3)	122 (25:75)	3.5 (99:1)

[a] No significant oxidation reaction has been observed. [b] Corresponding product obtained with selectivity >98%. [c] Product distribution of 70:2:28 for epoxide, glycol and glycol monomethyl ether. [d] Product selectivity in parentheses: sulfoxide/sulfone ratio.

Sn-beta had a much higher initial rate than Zr-beta for the BV reaction, whereas Ti-beta was inactive for this oxidation. Mechanistically, the BV oxidation of ketones with hydrogen peroxide (Scheme 1) involves two steps: addition of

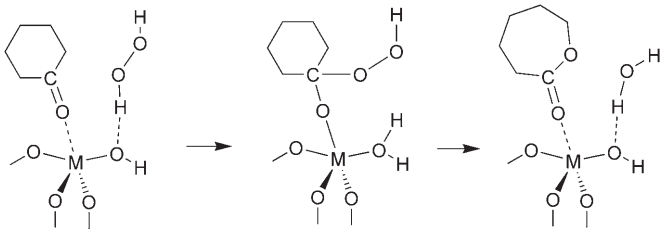

Scheme 1. BV oxidation of ketones with hydrogen peroxide.

H_2O_2 to the ketone to form a tetrahedral Criegee intermediate, and concerted rearrangement of this adduct to give the lactone product and water. The metal centre activates the carbonyl group of the ketone, making it more reactive towards the attack of the oxidant molecule.

The order of activity in the MPV reduction of cyclohexanone is quite similar to that of the BV oxidation: Sn-beta > Zr-beta ≫ Ti-beta. However, when benzaldehyde is employed as substrate in this reaction, the intrinsic activity is higher for Zr-beta than for Sn-beta; again, Ti-beta is inactive. The MPV reaction is a redox equilibrium catalysed by a Lewis acid (Scheme 2). The reaction has been generally supposed to proceed through a six-membered transition state in which both the ketone and the deprotonated alcohol are coordinated to the metal centre of a metal alkoxide cat-

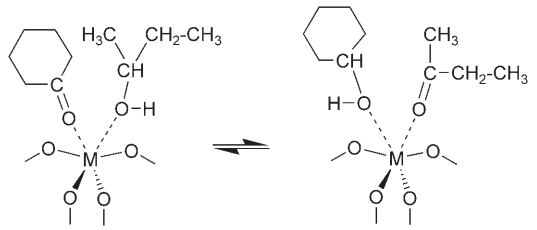

Scheme 2. MPV redox equilibrium catalysed by a Lewis acid.

alyst. The coordination of the ketone or aldehyde to the active site polarises and activates the carbonyl group, facilitating the hydride transfer from the alcohol.[13]

In octene epoxidation, it has been found that only Ti-beta possesses activity in the presence of hydrogen peroxide, whereas Sn- and Zr-beta are inactive. Interestingly, in the sulfide oxidation the activity of Zr-beta is similar to that of Ti-beta, but the selectivity towards the higher oxidation product, the sulfone, is higher for Zr-beta than for Ti-beta. Sn-beta does not exhibit any catalytic activity for this reaction. It seems clear that the mechanism of olefin epoxidation with H_2O_2 involves the adsorption of hydrogen peroxide on the Lewis acid centre and its activation to give a hydroperoxo species that will attack the olefin double bond. Although there has been discussion about which oxygen is transferred to the olefin, in a recent theoretical study[14] on propylene epoxidation catalysed by TS-1 the authors concluded that the mechanism proceeds by proximal oxygen abstraction (Scheme 3) and involves an electrophilic attack by this oxygen atom of the olefin C=C double bond. Similar activation of the hydrogen peroxide through formation of a hydroperoxo species should be the first step of the sulfide oxidation reaction.

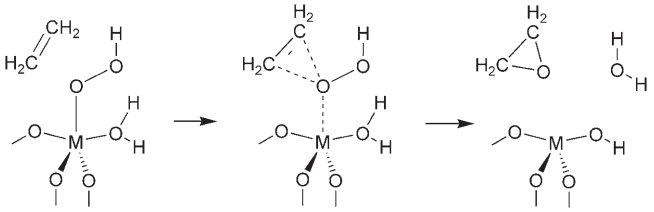

Scheme 3. Proximal oxygen abstraction mechanism of propylene epoxidation catalysed by TS-1.

Thus, we have here two types of reaction differing in the species that is activated initially. In the first, the hydrocarbon adsorption and activation on the Lewis acid site is a key step, and competes favourably with H_2O_2 for adsorption on the metal centre. The second type involves the adsorption and activation of H_2O_2 on the Lewis acid site. Although the active site for all the reactions is a Lewis acid, and even the same Lewis acid site, it would probably be difficult to find a single parameter capable of defining and explaining the reactivity of the metal Lewis acid as an oxidation site. Therefore, we will have to explore the relative contributions to the global catalytic process of the different parameters (acid strength, HSAB, electron density back-donation, electronic changes on the site generated by interaction with the reactant molecule) involved in the formation of the acid–base adducts with the substrate or the oxidant.

Lewis acidity and hard–soft character of the isolated active sites: As reported in experimental and spectroscopic studies, Ti, Zr and Sn are incorporated in the framework of beta zeolite in tetrahedral coordination.[8,9,10] The optimised M–O and M–Si distances in the substituted zeolites summarised in Table 2 are greater than the initial Si–O and Si–Si lengths, and decrease in the order Zr > Sn > Ti, reflecting the size of the incorporated metal atom. However, the M-O-Si angles do not change much on average.

Table 2. Average metal–oxygen, metal–silicon distances and metal-oxygen-silicon angles, orbital energies E and hardness of the isolated active site **I**.

	I-Si	I-Ti	I-Zr	I-Sn
$r(M{-}O)_{av}$ [Å]	1.620	1.792	1.963	1.881
$r(M{-}Si)_{av}$ [Å]	3.075	3.266	3.397	3.297
$\sphericalangle(M\text{-}O\text{-}Si)_{av}$ [°]	144.6	148.5	146.8	143.4
E_{HOMO} [eV]	−8.02	−8.01	−7.96	−7.95
E_{LUMO} [eV]	0.32	−2.20	−1.57	−1.50
hardness [eV]	8.34	5.81	6.39	6.45

If we take the LUMO energy of a system as a measure of its Lewis acid strength, the Lewis acidity of beta zeolite is increased considerably by incorporation of a metal in the framework. The LUMO of pure silica beta zeolite, which has no Lewis acid character, lies at 0.32 eV, and is a linear combination of the four antibonding σ* (Si–O) orbitals. The LUMO of Sn-beta zeolite has the same composition, but it is 1.82 eV lower in energy, in agreement with the Lewis acid properties reported for this catalyst. The LUMOs of Ti-beta and Zr-beta zeolites correspond to the d_{z^2} atomic orbital on the metal atom, and are 0.70 and 0.07 eV more stable, respectively, than that of Sn-beta. According to the LUMO energy criteria, Ti-beta should be the most acidic catalyst of the series and Zr- and Sn-beta should have a very similar acidity. In support of this prediction, it has been found that Ti-beta is active for the epoxidation of olefins, whereas Sn- and Zr-beta are not (see Table 1).

However, Table 1 also shows that the activity of Sn-beta for the BV oxidation of cyclohexanone with H_2O_2 and for the MPV reduction of cyclohexanone with 2-butanol is higher than that of Zr-beta, whereas Ti-beta is not active for these reactions. Thus, we have taken into consideration the HSAB principle and have approximated the chemical hardness η of the three catalysts and two adsorbates involved, in terms of the one-electron energies of the frontier molecular orbitals (HOMO and LUMO), using $\eta \approx E_{LUMO} - E_{HOMO}$.[15] The values in Table 2 indicate that Ti-beta is slightly softer than Zr- and Sn-beta, pure silica beta being the hardest material. Since the calculated hardness for cyclohexanone is 6.04 eV, the order Ti > Zr ≈ Sn could be expected for the interaction of cyclohexanone with the catalysts and for the ac-

tivity in the BV and MPV reactions. If we use the same rationale for epoxidation and sulfoxidation, the fact that hydrogen peroxide is a hard Lewis base ($\eta = 8.28$ eV) must be considered; according to the HSAB principle, only a weak interaction with Ti-beta should be expected. These predictions do not agree with the experimental results, so we conclude that the HSAB principle is the controlling parameter in none of the reactions studied.

Whereas the Lewis acid strength criterion based on the catalyst LUMO energy can explain, by itself and to a first approximation the order of activity observed for epoxidation of olefins and oxidation of sulfides, for the reactions (BV and MPV) in which adsorption of the reactant hydrocarbon molecule is the key activation step we need to take into consideration another factor, namely the electron density back-donation from the catalyst to the unoccupied orbitals of the organic reactant. Altogether, these results indicate that it is not always possible to obtain general rules relating reactivity with Lewis acid strength or hardness of the isolated active sites, and that the interactions between the substrate and the catalyst have to be analysed also.

Interaction with hydrogen peroxide as Lewis base: The mechanism of olefin epoxidation with H_2O_2 involves the adsorption of hydrogen peroxide on the Lewis acid centre and its activation to give a hydroperoxo species that will attack the olefin double bond. Table 3 summarises the optimised values of the most important geometric data, and the variation in the non-bonding orbital (NBO) occupancies and natural population analysis (NPA) atomic charges of H_2O_2 coordinated to the metal cluster (**II** in Figure 1) and the hydroperoxo species (**III** in Figure 1).

Hydrogen peroxide adsorption on the Lewis acid centre involves one electron density transfer from the occupied orbitals of H_2O_2 to the LUMO of the catalyst, and formation of two hydrogen bonds with the oxygen atoms directly bonded to the metal. The donor–acceptor interaction between H_2O_2 and the catalyst active site, given by the variation in the orbital occupancies $\Sigma_{occ.}$ in Table 3, is stronger in the case of Ti-beta than in Zr- and Sn-beta, in agreement with the smaller HOMO–LUMO energy gap calculated for **II-Ti**. The NBO analysis indicates that in all three complexes the electron density moves mainly from the p_z and to a lesser extent from the p_y orbitals of O_a, the d_{z^2} orbitals of the metal atom being the target orbitals in **II-Ti** and **II-Zr**. As a result, there is a decrease in the positive charge on the metal atom. In contrast, the positive charge on the Sn atom is increased slightly by adsorption of H_2O_2; this is the most peculiar characteristic of Sn-beta. The Sn atom cannot accept the electron density transferred from hydrogen peroxide and pushes it into the lobes of the σ*(Sn–O) orbitals located on the oxygen atoms. In agreement with this idea, the negative charge on the four oxygen atoms directly bonded to M is not changed significantly by adsorption of hydrogen peroxide on Ti- and Zr-beta, but increases by 0.015 *e* in Sn-beta. In summary, the Sn centre just acts as an electron pump. The optimised distances in Table 3 indicate that the H_a–O_w and H_b–O_y hydrogen bonds are quite similar in the three structures.

The interaction of hydrogen peroxide with the catalyst results in a polarization of the O_a–O_b bond. The negative charge on O_a increases slightly in **II-Ti** and to a greater extent in **II-Zr** and **II-Sn**, while the O_b atom suffers a decrease in its negative charge in all systems. The simultaneous and apparently contradictory electron density shift from the p_z and p_y orbitals on O_a and increase in the negative charge on the same O_a atom are explained by a polarization of the O_a–H_a bond. The positive charge on the two hydrogen atoms of H_2O_2 increases by adsorption on the Lewis acid centre, indicating that electron density is moving from the H atoms to the O atoms. But this charge variation is more pronounced in the case of H_a, thus explaining the increase in the negative charge on O_a.

To obtain the hydroperoxo species active in the epoxidation reaction, H_a in **II** is trans-

Table 3. Optimised distances of **II** and **III**, variation in the NBO occupancies Σ and in the NPA atomic charges *q* caused by hydrogen peroxide adsorption on the catalyst and formation of the hydroperoxo intermediate, and HOMO–LUMO energy difference $\Sigma E_{HOMO-LUMO}$.[a]

	II-Ti	II-Zr	II-Sn	III-Ti	III-Zr	III-Sn
r(M–O_a) [Å]	2.407	2.417	2.384	1.919	2.069	2.026
r(M–O_b) [Å]	3.332	3.349	3.315	2.931	2.271	2.841
r(O_a–O_b) [Å]	1.431	1.434	1.433	1.404	1.452	1.450
r(H_a–O_w) [Å]	2.162	2.217	2.040	0.989	0.984	0.990
r(H_b–O_y) [Å]	1.954	1.894	1.920			
r(H_a–O_b) [Å]	1.917	1.928	1.928	2.140	3.587	1.726
r(M–O_w) [Å]	1.824	1.997	1.919	2.036	2.232	2.165
$\Delta_{occ.}p_yO_a$ [e]	−0.021	−0.023	−0.011	−0.050	−0.021	−0.018
$\Delta_{occ.}p_zO_a$ [e]	−0.090	−0.074	−0.085	−0.182	−0.115	−0.035
$\Delta_{occ.}p_yO_b$ [e]	−0.004	−0.005	−0.005	−0.008	−0.021	−0.010
$\Delta_{occ.}p_zO_b$ [e]	−0.003	−0.004	−0.001	−0.045	−0.100	−0.048
$\Delta_{occ.}\sigma^*(O_a–O_b)$ [*e*]	0.010	0.011	0.010	0.013	0.001	0.009
$\Sigma_{occ.}$ [e]	−0.108	−0.095	−0.092	−0.272	−0.256	−0.104
Δq(O_a) [eV]	−0.003	−0.048	−0.055	0.026	−0.061	−0.131
Δq(O_b) [eV]	0.025	0.032	0.034	−0.029	−0.045	−0.050
Δq(H_a) [eV]	0.042	0.055	0.055	0.057	0.063	0.069
Δq(H_b) [eV]	0.018	0.027	0.021	0.032	0.025	0.036
Δq(M) [eV]	−0.075	−0.045	0.004	−0.122	−0.068	−0.033
$\Delta q(O_{x,y,z,w})_{av}$ [eV]	−0.003	−0.007	−0.015	0.005	0.014	0.028
$\Delta E_{HOMO-LUMO}$ [eV]	5.41	6.48	6.79	4.25	6.45	6.33

[a] For atom labelling, see Figure 1.

ferred to the O_w oxygen atom forming a water molecule coordinated to the metal centre. Among the several possible orientations of the −OOH group, which is able to form hydrogen bonds with different framework oxygen atoms, only **III** possesses an adequate geometry for the oxygen transfer and water formation needed in the epoxidation reaction. Therefore, the model **III** depicted in Figure 1 has been considered as the active species, in which H_b, O_b and H_a form the leaving water molecule, the O_a oxygen atom is transferred to the double bond to form the epoxide product and the rest of the atoms comprise the empty catalytic active site. The M–O_w bond lengths increase by 0.20–0.25 Å when **II** is converted into **III** (Table 3). At the same time, a covalent bond is formed between the metal atom and O_a, with M−O_a distances between 0.35 and 0.50 Å shorter in **III** than in **II**. A very particular interaction between the metal atom and O_b has been detected in the Zr–hydroperoxo system **III-Zr**, whose optimised geometry is depicted in Figure 2. The

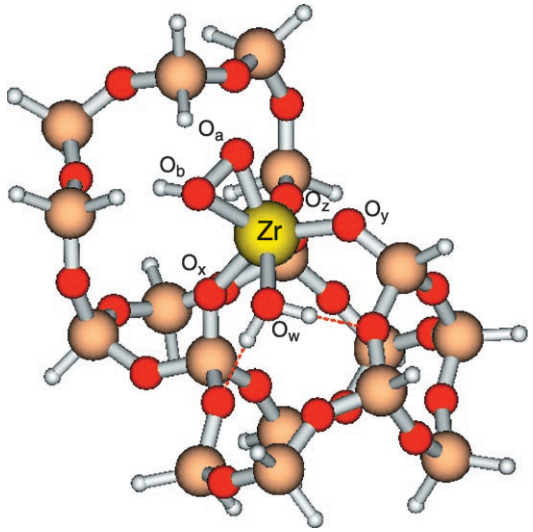

Figure 2. Optimised geometry of the Zr–hydroperoxo species **III-Zr**.

M−O_a and M−O_b distances are not too different, and the system could be better described as a η^2-peroxo complex. In agreement with this interpretation, the NBO analysis for **III-Zr** shows comparable values for the electron density transfer from the p_z orbitals of O_a and O_b to the metal atom, and similar values for the negative charges on O_a and O_b.

Since an electrophilic attack by the O_a atom on the π electrons of the C=C bond is postulated for the epoxidation mechanism, the atomic charge on O_a and the polarization of the O_a−O_b bond have been proposed as predictors of reactivity towards olefin epoxidation:[14] thus, the lower the negative charge on O_a and the greater the polarization or weakening of the O_a−O_b bond, which should be broken as the reaction proceeds, the higher the reactivity of the system. The negative charges on O_a and O_b are similar in Zr-beta and greater than in hydrogen peroxide, and therefore according to both criteria this catalyst is not active for olefin epoxidation, in agreement with the experimental results. In the case of the Sn-beta catalyst, the formation of the hydroperoxo intermediate results in slight changes in the electron distribution around the active site. Whereas during H_2O_2 adsorption the electron density transferred to the catalyst does not accumulate on the tin centre but is distributed further between among the framework oxygen atoms, the formation of a fifth Sn−O bond now induces a decrease in the positive charge on the tin atom. At the same time, the negative charge on the four $O_{x,y,z,w}$ atoms decreases, and that on O_a and O_b increases. As in Zr-beta, none of these changes polarises or weakens the O_a−O_b bond and the catalyst is inactive for olefin epoxidation.

The HOMO in all the structures **II** and **III** is similar, being a linear combination of the two p_z orbitals on the O_a and O_b atoms. But the composition and energies of the unoccupied molecular orbitals depicted in Figure 3 already suggest a different reactivity for Ti-beta. The HOMO–LUMO energy gap in **III-Ti** is only 4.25 eV and therefore the electron density transfer from hydrogen peroxide to the catalyst increases considerably when **II-Ti** is transformed into **III-Ti**. The occupancy of the molecular orbitals of the hydroperoxo fragment decreases by 0.272 e, and most of this electron density (0.182 e) comes from the p_z orbital on O_a. As a result, the O_a in **III-Ti** is more positively charged than in H_2O_2, and this system becomes capable of the electrophilic attack involved in the olefin epoxidation. Moreover, the σ*(O_a–O_b) antibonding orbital seems to be more activated by Ti-beta than by Zr- and Sn-beta catalysts. In **III-Sn**, the σ*(O_a-O_b) orbital lies at −0.24 eV, so it is considerably higher in energy than the LUMO of the system, which is a combination of the five σ*(Sn–O) antibonding orbitals. In Zr-beta, the σ*(O_a–O_b) orbital interacts favourably with the d_{xy} orbital on the metal atom, and is stabilised to −0.52 eV. The stabilizing interaction in Ti-beta between the σ*(O_a–O_b) orbital and the d_{z^2} orbital on Ti is more important, and the energy of the resulting molecular orbital is as low as −0.88 eV. Although the occupancy of the σ*(O_a–O_b) orbital in **III-Ti** is not significantly higher than in **III-Zr** or **III-Sn**, its lower energy makes it more accessible for interaction with the HOMO of the olefin.

This is in perfect accord with the experimental results for the epoxidation of octene. The only zeolite that was able to catalyse this reaction was Ti-beta; Sn- and Zr-beta were completely inactive (Table 1). Therefore, we can conclude that for the reactions involving H_2O_2 adsorption and activation on the Lewis acid site, the most influential parameter of the system is the positive charge on O_a, which is directly related to the ability of the metal to accept electron density from the peroxide fragment, and therefore to the acid strength criteria based on the catalyst LUMO energy.

Nevertheless, since the coordination of H_2O_2 to Zr-beta was found to be very unusual and similar to other homogeneous oxidants such as V/*t*BuOOH, a further oxidation reaction was chosen, namely sulfoxidation. This reaction is assumed to have lower activation energies, and could therefore provide a test reaction in which all three catalysts show

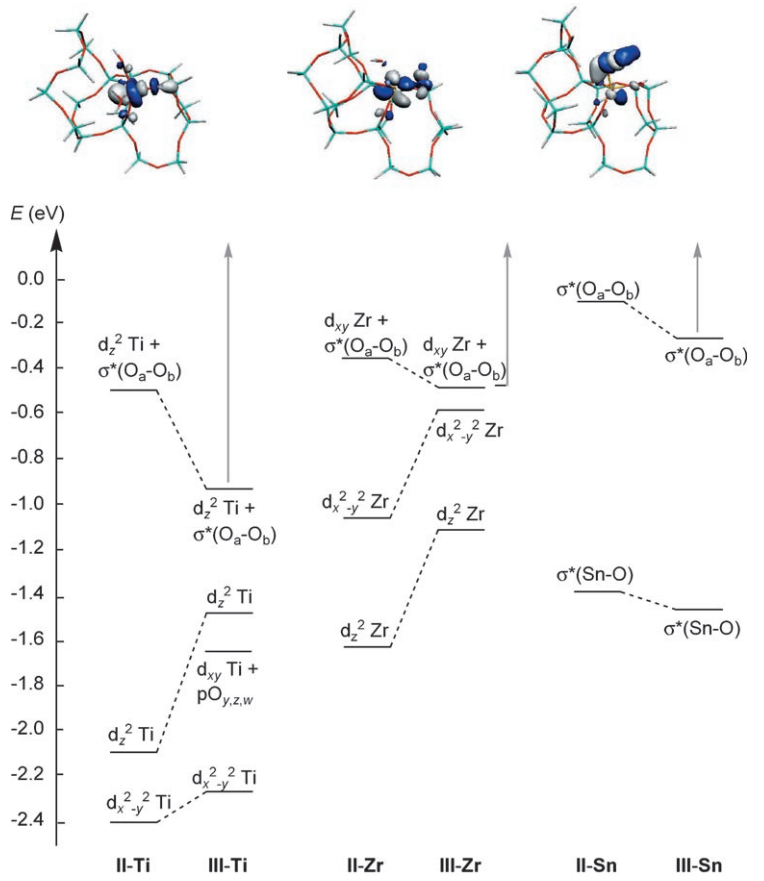

Figure 3. Energy of the LUMOs of **II** (adsorbed hydrogen peroxide) and **III** (metal–hydroperoxo species) calculated for Ti-, Zr- and Sn-beta catalysts, and composition of the $\sigma^*(O_a–O_b)$ orbital.

some catalytic activity. This was not the case for Sn-beta, but Zr-beta and Ti-beta gave similar initial reaction rates about one order of magnitude higher than the epoxidation rate with Ti-beta. The most surprising observation was that the product selectivity differed for the two catalysts and that the main product with Zr-beta was the sulfone, even at low conversions. This additional proof of the unusual hydrogen peroxide coordination and activation on the Zr centre is worth further study.

Interaction with carbonyl groups: back-donation effects: As discussed above, neither the acid strength given by the LUMO energy nor the hardness of the isolated Lewis acid sites can explain the order of activity observed for the (BV and MPV) reactions in which adsorption of the reactant hydrocarbon molecule was the key activation step. Therefore, the interaction between the reactants and the active site has been analysed in more detail, and the possibility of electron density back-donation from the catalyst to the organic molecule has been taken into consideration. It was explained above that the mechanism of these two reactions begins with adsorption of the ketone or the aldehyde on the catalyst active site. Table 4 summarises the most important geometric data, variation in the NPA atomic charges and NBO orbital occupancies of complexes **IV** (cyclohexanone coordinated to the metal cluster) and **V** (cyclohexanone and hydrogen peroxide coordinated to the metal cluster). Corresponding information concerning adsorption of benzaldehyde (**VI**) is given in Table 5.

Cyclohexanone (or benzaldehyde) adsorption on the Lewis acid centre involves two different donor–acceptor interactions: one electron density shift from the organic molecule to the metal centre and one back-donation from the catalyst to the antibonding $\pi^*(CO)$ orbital of the adsorbent. The NBO analysis indicates that

Table 4. Optimised distances of **IV** and **V**, variation in the NBO occupancies $\Delta_{occ.}$ and in the NPA atomic charges Δq caused by cyclohexanone adsorption on the catalyst, and energy difference between the $\pi^*(CO)$ orbital and the catalyst HOMO.[a]

	IV-Ti	IV-Zr	IV-Sn	V-Ti	V-Zr	V-Sn
$r(M–O_c)$ [Å]	2.235	2.298	2.230	2.181	2.279	2.173
$r(C–O_c)$[b] [Å]	1.232	1.237	1.240	1.236	1.240	1.244
$\sphericalangle$(M-O_c-C) [°]	135.5	138.9	133.3	137.2	140.0	135.7
$r(C–O_a)$ [Å]				3.114	4.035	2.916
$\Delta_{occ.} p_y O_c$ [*e*]	−0.049	−0.053	−0.031	−0.053	−0.056	−0.032
$\Delta_{occ.} p_z O_c$ [*e*]	−0.055	−0.024	−0.048	−0.064	−0.024	−0.058
$\Delta_{occ.} \pi(CO)$ [*e*]	−0.009	−0.010	0.001	−0.013	−0.012	0.001
$\Delta_{occ.} \pi^*(CO)$ [*e*]	0.039	0.053	0.054	0.047	0.058	0.070
$\Sigma_{occ.}$ [*e*]	−0.074	−0.034	−0.024	−0.083	−0.034	−0.019
$\Delta q(C)$ [*e*]	0.076	0.092	0.096	0.088	0.106	0.108
$\Delta q(O_c)$ [*e*]	−0.028	−0.095	−0.110	−0.039	−0.111	−0.137
$\Delta q(M)$ [e]	−0.108	−0.070	0.007	−0.099	−0.052	0.021
$\Delta q(O_{x,y,z,w})_{av}$ [*e*]	0.007	0.004	−0.013	0.000	−0.001	−0.016
$\Delta E_{(\pi^*(CO)–catalyst\ HOMO)}$ [eV]	6.35	5.70	5.78	6.05	4.26	5.67

[a] For atom labelling, see Figure 1. [b] $r(C–O_c)$ in cyclohexanone calculated at the same level of theory = 1.215 Å.

Table 5. Optimised distances of **VI**, variation in the NBO orbital occupancies and in the NPA atomic charges Δq caused by benzaldehyde adsorption on the catalyst, and energy difference between the π*(CO) orbital and the catalyst HOMO.[a]

	VI-Ti	VI-Zr	VI-Sn
r(M–O_c) [Å]	2.203	2.294	2.213
∢(M-O_c-C) [°]	127.1	127.7	125.5
r(C–O_c)[b] [Å]	1.235	1.241	1.244
r(C–H) [Å]	1.100	1.099	1.098
$\Delta_{occ.}p_yO_c$ [e]	−0.048	−0.047	−0.028
$\Delta_{occ.}p_zO_c$ [e]	−0.057	−0.020	−0.044
$\Delta_{occ.}\pi$(CO) [e]	−0.011	−0.012	−0.000
$\Delta_{occ.}\pi^*$(CO) [e]	0.047	0.065	0.068
$\Delta_{occ.}\sigma$(CH) [e]	−0.013	−0.015	−0.016
$\Sigma_{occ.}$ [e]	−0.082	−0.029	−0.020
Δq(C) [e]	0.046	0.059	0.051
$\Delta q(O_c)$ [e]	−0.028	−0.110	−0.113
Δq(H) [e]	0.061	0.073	0.075
$\Delta q(C_6H_5)$ [e]	0.068	0.090	0.094
Δq(M) [e]	−0.110	−0.067	−0.005
$\Delta q(O_{x,y,z,w})_{av}$ [e]	0.007	0.002	−0.005
$\Delta E_{(\pi^*(CO)-catalyst\ HOMO)}$ [eV]	5.10	4.74	4.71

[a] For atom labelling, see Figure 1. [b] r(C–O_c) in benzaldehyde (g) calculated at the same level of theory = 1.214 Å, r(C–H) = 1.114 Å.

the electron density moves mainly from the p_z and p_y orbitals on the carbonyl O_c atom and also from the π(CO) bond to the catalyst LUMO. In the case of benzaldehyde, there is also a non-negligible transfer from the antibonding σ*(CH) orbital, and, as a consequence, the r(C–H) bond length decreases from 1.114 Å in the gas phase to ~1.100 Å in complexes **VI**. The back-donation occurs between the HOMO of the catalyst, which is a combination of the lone pairs on the oxygen atoms of the cluster, and the LUMO of the organic molecule, which is the antibonding π*(CO) orbital on the carbonyl group.

For Ti- and Zr-beta, the electron density transferred from the occupied orbitals of cyclohexanone and benzaldehyde to the metal cluster is greater than that received by the organic molecule through back-donation. Consequently, the electron density on the titanium and the zirconium atoms increases and their positive charges decrease. Furthermore, polarization of the carbonyl bond can be detected, since both the positive charge at the carbon atom and the negative charge at the oxygen atom increase. Although the decrease in the occupancies $\Sigma_{occ.}$ of the cyclohexanone and benzaldehyde orbitals, and the polarization of the carbonyl groups (Δq(C) and $\Delta q(O_c)$), are very similar for Zr-beta and Sn-beta, the tin metal centre, behave quite differently. As already discussed for adsorption of H_2O_2, the tin atom cannot accept the transferred electron density and distributes this between the four next-neighbour oxygen atoms of the zeolite framework. Again, an increase in the negative charge on the $O_{x,y,z,w}$ atoms of Sn-beta is observed after adsorption of cyclohexanone (Table 4). This increase, however, is not so pronounced in the case of benzaldehyde (Table 5). Although the electron density transfer from the organic molecule to the catalyst is quite similar for cyclohexanone and benzaldehyde, comparison of NPA atomic charge variations in Tables 4 and 5 show differences between the two molecules. Thus, whereas the increase in the positive atomic charge on the C atom is close to 0.1 e in cyclohexanone, it is only about 0.05 e in benzaldehyde. The increase in the negative charge on the O_c atom is similar in both molecules, and the difference can be mainly related to the donating character of the benzaldehyde benzyl ring, which becomes positively charged after coordination to the catalyst active site.

The greatest decrease observed in the occupation of the cyclohexanone and benzaldehyde orbitals when they coordinate to the Ti centre could be expected for two reasons. On one hand, the LUMO of Ti-beta is the most stable (cf. Table 2) among the metal-substituted beta samples, and therefore the electron density shift from cyclohexanone or benzaldehyde to the metal centre, measured by the variation in the occupancies of the orbitals analysed, is higher than in Zr-and Sn-beta. On the other hand, the back-donation is energetically disfavoured for Ti-beta. As shown in Figure 4 for the case of cyclohexanone, the LUMO and LUMO+1 orbitals of the **IV-Ti** system are the d_{z^2} and $d_{x^2-y^2}$ atomic orbitals on Ti, and the cyclohexanone π*(CO) orbital appears at −1.14 eV, resulting in a π*(CO)–catalyst HOMO energy gap of 6.35 eV that makes the back-donation interaction very difficult. In contrast, the increase in the occupancy of the π*(CO) orbital given by the NBO analysis is greater in **IV-Sn** (0.054 e) and **IV-Zr** (0.053 e) than in **IV-Ti**, indicating a better back-donation in these two cases. Indeed, when cyclohexanone is adsorbed on Sn-beta, the σ*(SnO) orbital is strongly destabilised and the π*(CO) orbital becomes the LUMO of the **IV-Sn** system, resulting in a π*(CO)–catalyst HOMO energy gap of 5.78 eV (see Table 4) that is ≈0.5 e lower than for **IV-Ti**. In **IV-Zr**, the LUMO is a linear combination of the d_{z^2} atomic orbital on Zr and the π*(CO) molecular orbital on cyclohexanone, and the calculated energy gap is 5.70 eV, similar to that of **IV-Sn**.

The molecular orbital distribution of benzaldehyde adsorption complexes **VI** (not depicted) is quite similar to that of cyclohexanone adsorption complexes **IV**. In all three structures, the LUMO is a linear combination of the carbonyl π*(CO) orbital and three p_z orbitals on the two *ortho*- and one *para*-C atoms of the phenyl ring. The calculated orbital energies are −2.58, −2.92 and −2.92 eV for **VI-Ti**, **VI-Zr** and **VI-Sn**, respectively. Since the resulting energy differences between these orbitals and the catalyst HOMOs (Table 5), are about 1 eV lower than the corresponding values obtained for cyclohexanone, the back-donation is more important in this case, as reflected in the higher values of the π*(CO) orbital occupancy obtained for benzaldehyde.

The back-donation or electron density transfer from the catalyst to the antibonding π*(CO) molecular orbital of cyclohexanone or benzaldehyde weakens the carbonyl double bond and, as a result, the C–O distance increases and the ν_{CO} vibration frequency is shifted to smaller values. When cyclohexanone was adsorbed on Ti-, Zr- and Sn-beta catalysts, the $\Delta\nu_{CO}$ vibration frequency shifts measured by IR

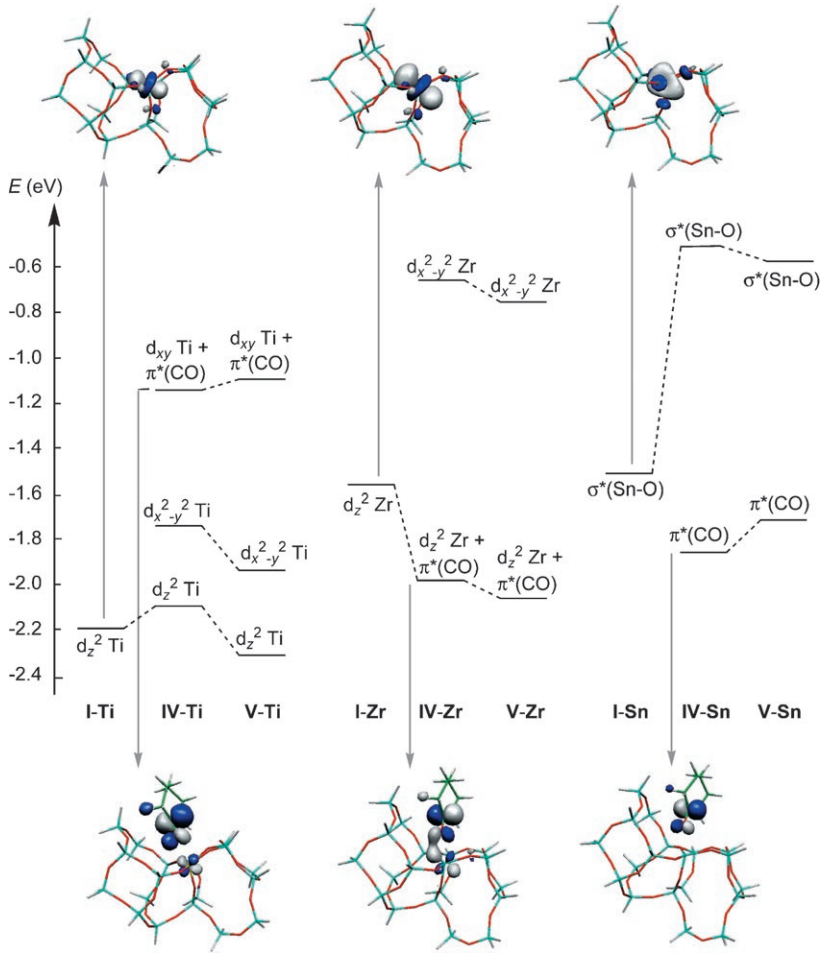

Figure 4. Energy of the LUMOs of **I** (isolated Lewis centres), **IV** (adsorbed cyclohexanone) and **V** (complex of reactants for the Baeyer–Villiger reaction) calculated for Ti-, Zr- and Sn-beta catalysts, and composition of the LUMO in **I** and the π*(CO) orbital in **IV**.

spectroscopy were −32, −42 and −48 cm^{-1} respectively.[9] These values indicate that the degree of cyclohexanone activation by the catalysts follows the order Ti < Zr < Sn, which is the order observed for the activity of the catalysts for the BV and MPV reactions.

When hydrogen peroxide coordinates to the O_w atom of the catalyst, as in **V-Ti**, **V-Zr** and **V-Sn**, to initiate the Baeyer–Villiger reaction, the HOMO of all the new systems is not located on the catalyst, but is a linear combination of the lone pairs or p_z orbitals on the O_a and O_b atoms of H_2O_2, so that the back-donation to the π*(CO) orbital of cyclohexanone occurs from the lone pair or p_z orbital on O_a. Since the π*(CO)–catalyst HOMO energy gap in structures **V** is smaller than in systems **IV**, there is a reinforcement of the back-donation interaction reflected in greater values of the occupancies of the π*(CO) orbital, in longer C–O_c distances, and in greater positive charges on the C atom. At the same time, there is a stabilization of the catalyst LUMO that causes an increase in the electron density transfer from cyclohexanone to the metal centre. This is reflected in a slight decrease in the occupancies of the cyclohexanone bonding and nonbonding orbitals, and causes a shortening of the M–O_c distances when going from **IV** to **V**. However, the behaviour of tin and zirconium catalysts cannot be explained only in terms of energetic criteria, because although the energy gap in **V-Zr** is considerably smaller than in **V-Sn**, the degree of back-donation is considerably greater in Sn-beta. As discussed in reference [16] for Sn-beta, the relative orientation of cyclohexanone and hydrogen peroxide in **V** strongly favours the overlap between the p_z orbital on O_a and the π*(CO) orbital of cyclohexanone. This is true for the case of Sn, for which the C–O_a calculated distance is 2.916 Å, but not for Zr, with a calculated value of r(C–O_a) of 4.035 Å. The difference in orbital overlap for Zr- and Sn-beta could explain the much better performance of Sn-beta in the BV reaction. Sn-beta has a much higher initial rate than Zr-beta, and Ti-beta is completely inactive for this oxidation (Table 1).

Since the mechanism of the MPV reaction involves a hydride transfer from the secondary C atom of the alcohol to which the hydroxyl group is bonded to the C atom of the carbonyl group, either the positive atomic charge on the carbonyl C atom or the polarization or weakening of the CO bond, related to the occupancy of the π*(CO) orbital, could be used as a predictor of reactivity towards the MPV reaction. Both criteria suggest a higher reactivity for the Zr- and Sn-beta catalysts, in agreement with the experimental results. However, whereas the initial rates measured for the MPV reaction of cyclohexanone with 2-butanol catalysed by Sn-beta are about 4.5 times higher than those catalysed by Zr-beta, when the reactant is benzaldehyde the reverse order is found, and the Zr-beta catalysed reaction is about 3.4 times faster than the Sn-beta catalysed one. This behaviour can be directly related only to the positive charge on the carbonyl C atom. The Δq(C) values calculated for adsorbed cyclohexanone (Table 4) follow the order **IV-Zr** < **IV-Sn**, whereas in the case of benzaldehyde (Table 5) the trend is **VI-Zr** > **VI-Sn**. In addition, for each catalyst, the Δq(C) values calculated for cyclohexanone are higher than those obtained for benzaldehyde, in agreement with the higher reaction rates observed for cyclohexanone reduction.

Activity prediction for other metal-containing catalysts: Once the parameters that describe the reactivity of the three Lewis acid catalysts studied were identified (the LUMO energy and the variation in the net atomic charge on the O_a atom to describe the epoxidation and sulfide oxidation reactions, and the C–O bond length and the net atomic charge on the carbonyl C atom in the BV and MPV reactions), we used them to predict the reactivity that other catalysts would possess if they could be obtained with different metal atoms tetrahedrally coordinated in framework positions of beta zeolite. Tetravalent Mo, Ru, Ge and Se, together with trivalent Sc and Ga, have been included in this theoretical study. For Sc and Ga, the negative charge generated in the framework by substitution of a tetravalent Si atom by a trivalent atom has been compensated with a proton.

The results summarised in Table 6 indicate that the strongest Lewis acids would be Ru- and Mo-beta catalysts, with calculated LUMO energies lower than −3.2 eV, followed by Ti- and Se-beta catalysts, whose LUMOs lie at approximately −2.0 eV. There is a correlation between the LUMO energy of the isolated active site **I** and the change in the net atomic charge on the O_a atom in the hydroperoxo intermediate **III**; that is, the more stable the catalyst LUMO, the higher the degree of electron density transfer from the organic fragment to the metal. As a result, the $\Delta q(O_a)$ in Mo- and Ru-beta systems is positive and greater than that obtained for Ti-beta. Therefore, if Mo^{IV} and Ru^{IV} could be introduced in the framework of beta zeolite, the resulting systems would be expected to show a large catalytic activity for olefin epoxidation and sulfide oxidation reactions.

The Lewis acid strength of the rest of the systems is lower than that of Zr- and Sn-beta, and therefore they are not supposed to be active for olefin or sulfide oxidations. Ge- and Ga-beta systems are the weakest Lewis acids, but the ability of the Ga-substituted system to activate cyclohexanone is not negligible. According either to the C–O bond length or to the positive charge on the C atom, the activity of Sc- and Ga-beta for the BV and MPV reactions should be similar to that of Zr-beta. However, neither Ge- nor Se-beta would be able to activate carbonyl groups. Mo- and Ru-beta are special cases. Except for these two systems, there is a linear correlation between the calculated C–O bond lengths and the positive charges on the C atom: the longer the C–O bond, the greater the positive charge on the C atom. But in **IV-Mo** and **IV-Ru**, the r(C–O) values suggest a degree of cyclohexanone activation even higher than that obtained for **IV-Sn**, whereas the calculated q(C) values are among the lowest. The reason is related to the partially filled d shell of these two atoms. Except for Mo- and Ru-substituted systems, the HOMO in **IV** is localised on the framework oxygens, and the π*(CO)–HOMO energy difference is greater than 5.7 eV. In **IV-Mo** and **IV-Ru**, the catalyst HOMO is a d orbital on the metal centre, and the calculated π*(CO)–HOMO energy difference is considerably smaller: 3.44 eV for **IV-Mo** and 4.44 eV for **IV-Ru**. This produces a greater degree of electron density transfer from the catalyst to cyclohexanone, which is reflected not only in the lengthening of the C–O bond but also in the less positive atomic charges. Since q(C) is the most important descriptor of reactivity for BV and MPV reactions, neither Mo- nor Ru-beta should be expected to be active for this type of reaction.

Conclusion

The catalytic activity of Brönsted acids has frequently been correlated with their intrinsic acid strength, that is, to their ability to form acid–base adducts through proton transfer. In contrast, in the case of Lewis acids as catalysts for oxidation reactions there is only a certain degree of electron density transfer from the base to the acid. It has been observed that the parameters to be considered in order to describe the more complicated Lewis acid–base interaction are: the intrinsic acid strength of the active site; the back-donation from the Lewis acid to the empty orbitals of the base; and the changes in the electronic levels of the active site caused by its interaction with the reactant molecules.

It has been found that for those reactions involving adsorption and activation of H_2O_2 on the Lewis acid site to give a hydroperoxo species, the activity of the catalyst is directly related to its acid strength measured as LUMO energy. Thus, the lower the LUMO energy, the greater the electron density transfer from the peroxide fragment to the metal and therefore the higher the catalyst activity. However, for those reactions in which the species initially adsorbed and activated is the hydrocarbon, the acid strength criteria based on the LUMO energy cannot explain the order of activity. In these cases, the hydrocarbon is not directly bonded but only coordinated to the metal, and the electron density back-donation and the electronic changes in the active site become key factors to de-

Table 6. Calculated parameters for other metal-containing models of Sn-beta zeolite: LUMO energy and nature of the isolated active site **I**, variation in the NPA atomic charges q on the O_a atom in the peroxide species **III**, and CO optimised bond lengths and NPA atomic charges on the C atom in the cyclohexanone adsorption complexes **IV**.

	I		**III**	**IV**	
M	E_{LUMO} [eV]	LUMO	$\Delta q(O_a)$ [e]	r(C–O) [Å]	q(C) [e]
Sc^{III}	−1.15	d_{z^2} Sc		1.237	0.678
Ti^{IV}	−2.20	d_{z^2} Ti	0.025	1.232	0.668
Zr^{IV}	−1.57	d_{z^2} Zr	−0.061	1.237	0.684
Mo^{IV}	−3.28	$d_{x^2-y^2}$ Mo	0.071	1.242	0.639
Ru^{IV}	−3.41	$d_{x^2-y^2}$ Ru	0.224	1.240	0.657
Ga^{III}	−0.12	σ*(Ga–O)		1.237	0.681
Ge^{IV}	−0.29	σ*(Ge–O)		1.225	0.639
Sn^{IV}	−1.50	σ*(Sn–O)	−0.132	1.240	0.688
Se^{IV}	−2.01	p Se	−0.013	1.226	0.634

scribe the acid–base interaction. It has been found that the back-donation to the π^*(CO) orbital causes an increase in the C–O bond lengths, a shift to lower values of the ν_{CO} vibration frequencies (calculated and measured experimentally) and an increase in the positive charge on the carbonyl C atom. Although all these variables are related, it has been found that only the q(C) charge can explain the activity of all catalysts for the BV and the MPV reactions for cyclohexanone and benzaldehyde.

Taking into account the variables that have been found to determine the catalytic activity for each type of reaction, the behaviour of several metal-substituted hypothetical catalysts has been predicted.

Experimental Section

Models and methods: The catalytic activity of Ti-, Zr- and Sn-containing zeolites is related to the presence of isolated tetrahedral M^{IV} atoms in framework positions. Metal incorporation is energetically disfavoured because it causes important geometric distortion around the substituting atom, due to the greater size of MO_4 compared to tetrahedral SiO_4. In the presence of water and under suitable conditions, the hydrolysis of one or more M–O–Si bonds can occur, resulting in a local relaxation of the structure at the M sites. Moreover, during the adsorption process, the metal atom has to interact with the reactants and increase its coordination number; this will be easier in the more flexible partially hydrolysed sites. Previous theoretical and spectroscopic work[16,17] showed that the active sites in the Sn-beta catalysed Baeyer–Villiger oxidation of cyclic ketones are framework tin centres with one hydrolysed Sn–O–Si bond. Similarly, it was found that Ti sites adjacent to Si vacancies in TS-1 lattices, and therefore having at least one Ti–OH bond, are more reactive for propylene epoxidation than fully coordinated Ti sites.[14,18] Therefore, a model with one hydrolysed M–O–Si bond (**I** in Figure 1) has been used in this work to simulate the Lewis acid centres.

To determine an adequate size for the cluster of atoms used to simulate the Lewis acid centres that would be adequate, we have performed a series of preliminary calculations on the interaction betweeen cyclohexanone and the Sn-beta active site using clusters that included two, three and four coordination spheres around the Sn atom. The results obtained with the larger model were in agreement with experiments, and therefore a cluster of atoms containing a Si atom in the T9 position ($Si_{(T9)}$) and four coordination spheres around it was cut out from the periodic structure of pure silica beta zeolite,[19] and one of the $Si_{(T9)}$–O–Si(–O)$_3$ groups was substituted by a $Si_{(T9)}$–O–H group. The dangling bonds that connected the cluster to the rest of the solid were saturated with H atoms at 1.49 Å from the Si atoms and orientated towards the positions occupied in the crystal by the oxygen atoms in the next coordination sphere; the result was a model with 68 atoms. Then, the $Si_{(T9)}$ atom was substituted by Ti, Zr and Sn to give models **I-Ti**, **I-Zr** and **I-Sn**, respectively. The other structures in Figure 1 were obtained by coordinating hydrogen peroxide (**II**), cyclohexanone (**IV**), and cyclohexanone plus H_2O_2 (**V**)as reactants for the BV process, and benzaldehyde (**VI**) on models **I**, whereas **III** was obtained from **II** through deprotonation and reorientation of H_2O_2.

The geometries of all the structures in Figure 1 were optimised by means of the ONIOM scheme[20,21] as implemented in the Gaussian 03 computer program.[22] The ONIOM approach subdivides the *real* system into a *model* system, which is described at the highest level of theory, and subsequent parts or layers which are computed at progressively lower and computationally cheaper levels of theory. In this work, the model system included the M atom, the four oxygen atoms in the first coordination sphere, the Si or H atoms bonded to them and the adsorbed molecules. The coordinates of these atoms were completely optimised with the density functional B3PW91 method[23,24] using a LANL2DZ effective core potential basis set for Ti,[25] Zr[25] and Sn,[26] and the standard 6-31G(d,p) basis set[27] for C, O, Si and H atoms. The rest of the system was treated at the Hartree–Fock level using the 3-21G basis set,[28–33] and only the coordinates of the terminal H atoms were kept fixed at their original positions. The combination of levels of theory (DFT/DZP:HF/3-21G) and the size of the model system chosen for the ONIOM calculations has been reported to provide results in excellent agreement with those obtained with full DFT periodic calculations.[34] Finally, orbital energies and occupancies and atomic charges were produced by natural bond orbital (NBO) methods.[35] These electronic properties were obtained from full DFT calculations in which all the atoms of the model were treated at the previously described B3PW91 level.

Catalyst preparation: The beta catalysts were prepared in fluoride media following literature procedures[9,10,36,37] and were calcined at 853 K for 3 h. The zeolites showed high crystallinity, and no peaks of SnO_2, TiO_2 or ZrO_2, respectively, were found by XRD. Nitrogen adsorption experiments on the calcined beta samples gave an isotherm very similar to that of pure silica beta with a micropore volume of 0.21 $cm^3 g^{-1}$ and BET surface areas of 450–475 $m^2 g^{-1}$. Silicon/metal ratios obtained from the metal contents determined by atomic absorption were: Si/Sn 108:1, Si/Ti 132:1, Si/Zr 116:1.

Catalytic reactions

Baeyer–Villiger (BV) oxidations: Cyclohexanone (108 mg) was mixed with aqueous hydrogen peroxide (136 mg, 35 %)and dioxane (3.0 g). A sample (50 mg) of the catalyst was added and the reaction mixture was heated to 90 °C for 1 h. The progress of the reaction was monitored by gas chromatography (HP-5 column, 15 m × 0.32 mm, 0.5 μm with a suitable temperature program). The initial rates were calculated after 5 and 15 min reaction time for Sn- and Zr-beta, respectively.

Meerwein–Ponndorf–Verley (MPV) reductions of cyclohexanone: A portion (3.42 g) of a stock solution prepared from cyclohexanone (855 mg) and 2-butanol (33.36 g) was placed in a round-bottom flask and a sample of the catalyst (7.5 mg Sn-beta, Zr-beta; 40 mg Ti-beta) was added. The progress of the reaction was monitored by gas chromatography (HP-5 column, 15 m × 0.32 mm, 0.5 μm with a suitable temperature program). The initial rates were calculated after 5, 15 and 240 min reaction time for Sn-, Zr- and Ti-beta, respectively.

Meerwein–Ponndorf–Verley (MPV) reductions of benzaldehyde: A sample of the catalyst (50 mg) was added to benzaldehyde (136 mg) and 2-butanol (3.34 g) in a round-bottom flask. The reaction mixture was stirred vigorously and heated to 100 °C. The progress of the reaction was monitored by gas chromatography (HP-5 column, 15 m × 0.32 mm, 0.5 μm with a suitable temperature program). The initial rates were calculated after 15, 5 and 120 min reaction time for Sn-, Zr- and Ti-beta, respectively.

Epoxidation of 1-octene: Octene (94 mg), hydrogen peroxide (23 mg, 35 %), nonane (7.0 mg; internal standard) and methanol (607 mg) were mixed in a 5-mL vial and a sample of the catalyst (5 mg) was added. The reaction mixture was stirred vigorously and heated to 60 °C. The progress of the reaction was monitored by gas chromatography (HP-5 column, 15 m × 0.32 mm, 0.5 μm with a suitable temperature program). The initial rate for Ti-beta was calculated after 30 min reaction time. For Sn- and Zr-beta no conversion could be detected at this reaction time.

Sulfoxidation of diphenyl sulfide: A sample of the catalyst (50 mg) was added to a mixture of diphenyl sulfide (572 mg), aqueous hydrogen peroxide (115 mg, 35 %) and acetonitrile (3.01 g) in a round-bottom flask. The progress of the reaction was monitored by gas chromatography (Carbowax column, 15 m × 0.32 mm, 0.5 μm with a suitable temperature program). The initial rates were calculated after 5 min for Ti- and Zr-beta, and after 45 min for Sn-beta.

Acknowledgements

Thanks are given to CICYT (MAT-2006–3798164) for financial support and the Universitat de Valencia for computing facilities. M.R. is grateful

to the Spanish Ministry of Science and Technology for a "Ramón y Cajal" fellowship.

[1] A. Corma, *Catal. Rev. Sci. Eng.* **2004**, *46*, 369–417.
[2] A. Corma, H. Garcia, *Chem. Rev.* **2003**, *103*, 4307–4365.
[3] M. Taramaso, G. Perego, B. Notari, US 4410501, **1983**.
[4] P. Ingallina, M. G. Clerici, L. Rossi, G. Bellussi, *Stud. Surf. Sci. Catal.* **1995**, *92*, 31–39.
[5] A. Corma, H. Garcia, *Chem. Rev.* **2002**, *102*, 3837–3892.
[6] P. Wu, Y. Liu, M. He, T. Tatsumi, *J. Catal.* **2004**, *228*, 183–191.
[7] A. Corma, J. L. Jorda, M. T. Navarro, F. Rey, *Chem. Commun.* **1998**, 1899–1900.
[8] N. K. Mal, A. V. Ramaswamy, *Chem. Commun.* **1997**, 425–426.
[9] M. Renz, T. Blasco, A. Corma, R. Jensen, L. T. Nemeth, *Chem. Eur. J.* **2002**, *8*, 4708–4717.
[10] Y. Zhu, G. Chuah, S. Jaenicke, *J. Catal.* **2004**, *227*, 1–10.
[11] A. Corma, L. T. Nemeth, M. Renz, S. Valencia, *Nature* **2001**, *412*, 423–425.
[12] R. G. Parr, R. G. Pearson, *J. Am. Chem. Soc.* **1983**, *105*, 7512–7516.
[13] C. F. de Graaw, J. A. Peters, H. van Bekkum, J. Huskens, *Synthesis* **1994**, 1007–1017.
[14] D. H. Wells Jr., W. N. Delgass, K. T. Thomson, *J. Am. Chem. Soc.* **2004**, *126*, 2956–2962.
[15] R. G. Parr, W. Yang, *Density Functional Theory of Atoms and Molecules*, Oxford University Press, New York, **1989**.
[16] M. Boronat, A. Corma, M. Renz, G. Sastre, P. M. Viruela, *Chem. Eur. J.* **2005**, *11*, 6905–6915.
[17] M. Boronat, P. Concepcion, A. Corma, M. Renz, S. Valencia, *J. Catal.* **2005**, *234*, 111–118.
[18] D. Gleeseon, G. Sankar, C. R. A. Catlow, J. M. Thomas, G. Spano, S. Bordiga, A. Zecchina, C. Lamberti, *Phys. Chem. Chem. Phys.* **2000**, *2*, 4812–4817.
[19] J. M. Newsam, M. M. J. Treacy, W. T. Koetsier, C. B. de Gruyter, *Proc. R. Soc. London Ser. A* **1988**, *420*, 375–405.
[20] M. Svensson, S. Humbel, R. D. J. Froese, T. Matsubara, S. Sieber, K. Morokuma, *J. Phys. Chem.* **1996**, *100*, 19357–19363.
[21] S. Humbel, S. Sieber, K. Morokuma, *J. Chem. Phys.* **1996**, *105*, 1959–1967.
[22] M. J. Frisch, G. W. Trucks, H. B. Schlegel, et al., *Gaussian 03*, Revision B.04, Gaussian, Inc., Pittsburgh, PA, **2003**.
[23] J. P. Perdew, Y. Wang, *Phys. Rev. B* **1992**, *45*, 13244–13249.
[24] A. D. Becke, *J. Chem. Phys.* **1993**, *98*, 5648–5652.
[25] P. J. Hay, W. R. Wadt, *J. Chem. Phys.* **1985**, *82*, 270–283.
[26] W. R. Wadt, P. J. Hay, *J. Chem. Phys.* **1985**, *82*, 284–298.
[27] P. C. Hariharan, J. A. Pople, *Theor. Chim. Acta* **1973**, *28*, 213–222.
[28] J. S. Binkley, J. A. Pople, W. J. Hehre, *J. Am. Chem. Soc.* **1980**, *102*, 939–947.
[29] M. S. Gordon, J. S. Binkley, J. A. Pople, W. J. Pietro, W. J. Hehre, *J. Am. Chem. Soc.* **1982**, *104*, 2797–2803.
[30] W. J. Pietro, M. M. Francl, W. J. Hehre, D. J. Defrees, J. A. Pople, J. S. Binkley, *J. Am. Chem. Soc.* **1982**, *104*, 5039–5048.
[31] K. D. Dobbs, W. J. Hehre, *J. Comput. Chem.* **1986**, *7*, 359–378.
[32] K. D. Dobbs, W. J. Hehre, *J. Comput. Chem.* **1987**, *8*, 861–879.
[33] K. D. Dobbs, W. J. Hehre, *J. Comput. Chem.* **1987**, *8*, 880–893.
[34] X. Solans-Monfort, M. Sodupe, V. Branchadell, J. Sauer, R. Orlando, P. Ugliengo, *J. Phys. Chem. B* **2005**, *109*, 3539–3545.
[35] E. D. Glendening, A. E. Reed, J. E. Carpenter, F. Weinhold, *NBO,* Version 3.1, Theoretical Chemistry Institute, University of Wisconsin, Madison, WI, **1993**..
[36] T. Blasco, M. A. Camblor, A. Corma, P. Esteve, A. Martínez, C. Prieto, S. Valencia, *Chem. Commun.* **1996**, 2367–2368.
[37] T. Blasco, M. A. Camblor, A. Corma, P. Esteve, J. M. Guil, A. Martínez, J. A. Perdigón-Melón, S. Valencia, *J. Phys. Chem. B* **1998**, *102*, 75–88.

Received: April 5, 2006
Revised: May 4, 2006
Published online: August 25, 2006

